Near-Barrier Fusion of the ^{8}B+^{58}Ni Proton-Halo System

E. F. Aguilera *et al.*

Phys. Rev. Lett. **107**, 092701 — Published 24 August 2011

DOI: 10.1103/PhysRevLett.107.092701

Near-barrier fusion of the ^{8}B + ^{58}Ni proton-halo system.

E. F. Aguilera*, P. Amador-Valenzuela, E. Martinez-Quiroz, D. Lizcano, P. Rosales, H. García-Martínez, and A. Gómez-Camacho

Instituto Nacional de Investigaciones Nucleares, Apartado Postal 18-1027, DF-11801, México

J. J. Kolata, A. Roberts, L.O. Lamm†, and G. Rogachev‡

Physics Department, University of Notre Dame, Notre Dame, IN, 46556-5670, USA

V. Guimarães

Instituto de Fisica, Universidade de Sao Paulo, P. O. Box 66318, 05389-970, Sao Paulo, SP, Brazil

F. D. Becchetti, A. Villano§, M. Ojaruega, M. Febbraro, Y. Chen, and H. Jiang

Physics Department, University of Michigan, Ann Arbor, MI, 48109-1120, USA

P. A. DeYoung, G.F. Peaslee, C. Guess, and U. Khadka

Hope College, Holland, MI, 49422-9000, USA

J. Brown

Physics Department, Wabash College, P.O. Box 353, Crawfordsville, IN, 47933, USA

J. D. Hinnefeld

Physics Department, Indiana University South Bend, South Bend, IN, 46694-7111, USA

L. Acosta

Universidad de Huelva, E-21071 Huelva,

* eli.aguilera@inin.gob.mx

† deceased

‡ Present address: Florida State University

§ Present address: University of Minnesota

Spain and LNS-INFN, I-95123 Catania, Italy

E. S. Rossi Jr

UNIFIEO - Centro Universitário FIEO - CEP 06020-190, Osasco-SP, Brazil

J. F. P. Huiza

Departamento de Química e Exatas,

Universidade Estadual do Sudoeste da Bahia, 45206-190 Bahia, Brazil

T. L. Belyaeva

Universidad Autónoma del Estado de México,

Código Postal 50000, Toluca, México

Abstract

Fusion cross sections were measured for the exotic proton-halo nucleus ^{8}B incident on a ^{58}Ni target at several energies near the Coulomb barrier. This is the first experiment to report on the fusion of a proton-halo nucleus. The resulting excitation function shows a striking enhancement with respect to expectations for normal projectiles. Evidence is presented that the sum of the fusion and breakup yields saturates the total reaction cross section.

PACS numbers: 25.60.-t, 25.60.Pj , 25.70.-z

Much experimental and theoretical effort has lately been dedicated to investigating nuclear interactions of exotic neutron-halo nuclei[1–3]. As a consequence of the weak binding between the core and the halo, very large direct reaction cross sections occur for these systems at near-Coulomb-barrier energies. For instance, for the neutron halo system ^{6}He+^{209}Bi, the inclusive transfer/breakup cross section dominates the fusion yield in a >7 MeV wide region near to and below the barrier[4, 5]. The sum of fusion plus transfer/breakup yields saturates the total reaction cross section, which is also enhanced with respect to normal systems in this energy region. In contrast to the situation for neutron-halo projectiles, data on reactions of proton-halo systems are still scarce. The nucleus ^{8}B, adjacent to the proton drip line and possessing a very small proton separation energy of 0.138 MeV, has recently been studied in this context. An angular distribution for the breakup of ^{8}B on a ^{58}Ni target was measured at a single near-barrier energy[6]. It was found that Coulomb-nuclear interference at very large distances played an important role in the reaction mechanism because of the proton-halo nature of the projectile. More recently, elastic scattering measurements for the same system provided an excitation function for the total reaction cross section at near- and sub-barrier energies[7]. Remarkably, the "reduced" total reaction cross section, when plotted as a function of the "reduced" energy, is found to be virtually identical to that for ^{6}He on several targets[7], despite important differences in structure, binding energy, and reaction mechanisms for these two projectiles.

While the large reaction cross sections observed for neutron-halo systems have been shown to be related to the corresponding neutron transfer channels[8], projectile breakup is the most important direct process in the proton-halo case [7, 9]. However, in contrast with this clear predominance of direct reactions for the case of neutron halo systems, the breakup yield for ^{8}B + ^{58}Ni is far from saturating the corresponding total reaction cross section. One or more additional mechanisms must therefore make important contributions to the total reaction yield. The aim of this work is a precise identification of the most relevant reaction mechanisms involved in the interactions of proton halo systems. For this purpose, the fusion cross sections for ^{8}B+^{58}Ni have been measured at energies near to and below the Coulomb barrier. Comparisons are made with the total reaction cross section, breakup, and transfer data. A very preliminary version of some of the obtained data was given in Ref. [10].

The ^{8}B beams were generated using the ^{3}He(^{6}Li,^{8}B) reaction at the *TwinSol* facility[11] at the University of Notre Dame. Primary ^{6}Li^{3+} beams with energies between 31 and 38

TABLE I: Beam energies for the four stages (MeV). The incident (lab) energy, the cm energy at the center of the target, and the effective fusion energy from the iterative averaging procedure (see text) are listed for each run. Runs 6 and 7 were averaged for the E_{fus}=23.3 MeV point.

Run	Stage	E_{lab}	E_{cm}	E_{fus}	Run	Stage	E_{lab}	E_{cm}	E_{fus}
1	3	22.4	15.2	18.9	7	1	27.5	23.3	23.4
2	4	23.9	19.4	20.1	8	2	27.6	23.6	23.7
3	3	24.6	21.1	21.1	9	4	28.6	23.7	23.8
4	4	26.5	21.7	22.1	10	2	29.1	25.0	25.0
5	2	25.8	22.0	22.1	11	1	30.0	25.5	25.6
6	3	26.9	23.2	23.2					

MeV produced the ^{8}B beams listed in Table I. Primary beam currents for the different stages varied from 50 to 220 particle-nanoamperes (pnA), yielding secondary beam rates of 0.5-2.7$\times$ 10^4 s^{-1}. Several ΔE-E silicon surface-barrier telescopes were used at backward angles to detect protons evaporated from the fused system. Protons from ^{8}B breakup do not reach the detectors at these angles[12]. Two additional detectors at forward angles served to monitor the beam.

The secondary beam from *TwinSol* is generally contaminated by unwanted ions having the same magnetic rigidity. A bunched beam was used in order to identify the reaction products of interest, and to reject direct protons, by time-of-flight. Because of their partial time overlap with the ^{8}B beam, the most relevant contaminants and typical yields (relative to ^{8}B) were $^3He^{2+}$($\sim$45%) and $^7Li^{3+}$($\sim$45%). The beam energy resolution varied between 0.8 - 1 MeV (FWHM), and the time resolution was 4.7 - 9.4 ns. Although the effective beam spot size on target is about 4 mm, even a faint beam halo interacting with the target frame (diameter$\approx$25 mm) can produce substantial amounts of background protons that reach the telescopes. It was because of these background problems, and the low beam rates for bunched beams at *TwinSol*, that the experiment was performed in four stages (see Table I). In the first stage, three telescopes at 120^o, 135^o and 150^o and a 1.36 mg/cm^2 natural Ni target were used. For the second stage, the target was enriched ^{58}Ni (0.924 mg/cm^2) and an additional telescope at 105^o was included. No background measurements were made in

these two stages. In the third stage, the four telescopes were placed at 112.5°, 127.5°, 142.5°, and 157.5° and two targets were used. The first of these was an enriched ^{58}Ni target (0.725 mg/cm^2) mounted on a circular frame 25 mm in diameter made with the same size and from the same material as the frames used in stages 1 and 2. Measurements at E_{lab} = 24.6 and 26.9 MeV were made with this target. The second target, used for the measurement at E_{lab} = 22.4 MeV, was a natural Ni foil (5.60 mg/cm^2) mounted on a 13 cm×13 cm square frame. A natural Ni target was also used in the fourth stage, but the thickness was 2.22 mg/cm^2 and the frame dimensions were 8.9 cm×8.9 cm. The telescope positions were the same as in stage 3. The monitor detectors (telescopes for stages 1 and 2, single detectors for stages 3 and 4) were placed symmetrically at ±45°, except for stage 1 where they were at +45° and -60°.

Background determinations were performed during stages 3 and 4 by using pairs of identical target frames. One of them had no target and was used for blank target measurements right after the respective runs with a target. No modifications of the setup or the beam conditions were made. In addition to providing the proper corrections for the data taken in stages 3 and 4, these blank-target data showed a smooth energy dependence that could then be used to estimate a background correction for the measurements of stages 1 and 2.

In order to determine the contributions of the ^{7}Li and ^{3}He contaminant beams to the proton yields, additional experiments were performed to measure protons produced by these two projectiles on a ^{58}Ni target. The laboratory energies at the center of the target were 10.2, 11.1, and 12.1 MeV for ^{7}Li and 10.2, 11.5, and 12.7 MeV for ^{3}He. The detector telescopes were placed at 120°, 135°, 150°, and 165° while monitor telescopes were placed at ±45°. As it turned out, the ^{7}Li component was not a concern because the ^{7}Li beam energies were always well below the Coulomb barrier. This, combined with the fact that proton multiplicities for ^{7}Li + ^{58}Ni are about a factor of 2 lower than those for ^{8}B + ^{58}Ni, leads to a negligible effect (≈1%) on the proton yields. However, a contribution of up to 10% coming from the ^{3}He beam component was corrected for in a few cases. A typical proton spectrum is shown in Fig. 1.

Fusion cross sections were computed from the proton yields using multiplicities calculated with the code PACE [13]. Appropriate corrections were introduced to account for the respective isotopic composition when natural Ni targets were used. The repeat point at E_{fus} = 22.1 MeV, which was taken first using a ^{58}Ni target and later with a natural Ni

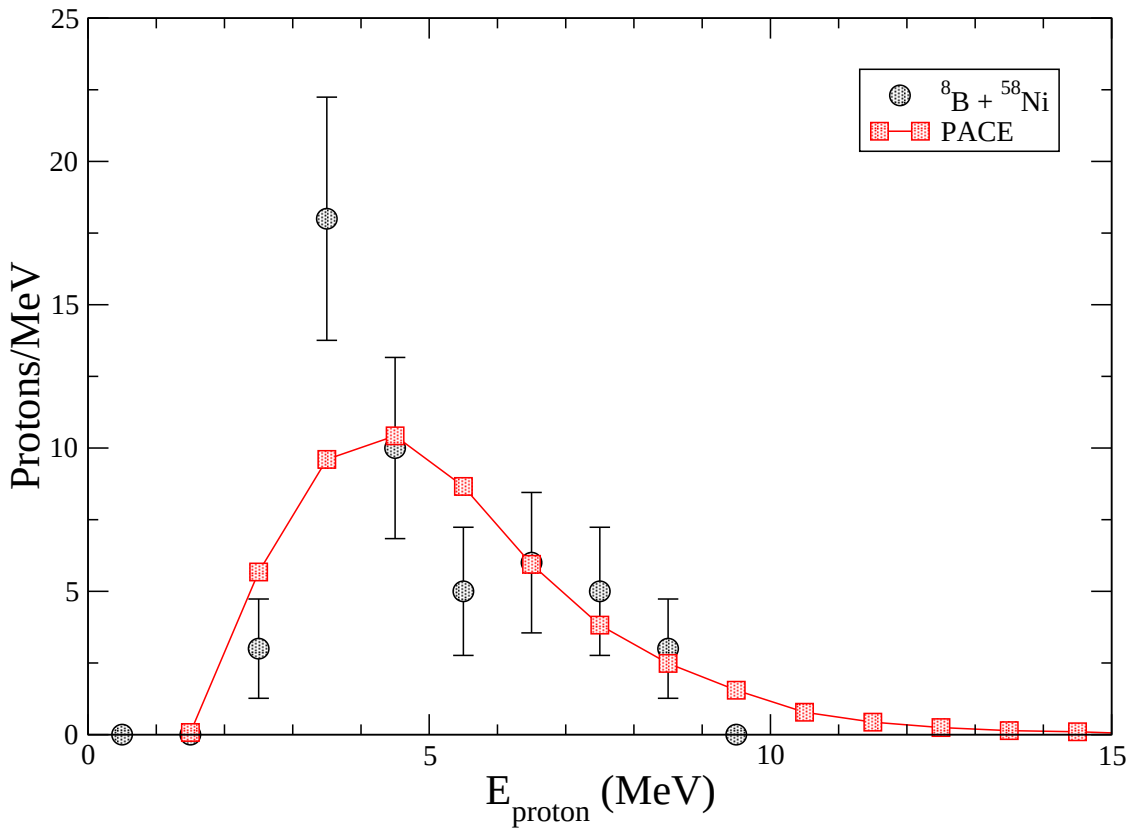

FIG. 1: Typical proton spectrum (E_{lab} = 22.4 MeV) compared with a PACE calculation. Data from all four telescopes have been summed and background corrections discussed in the text have been made.

target, validates the correction procedure. Model dependency was tested by varying the level density parameter a within extreme values ($A/10 \leq a \leq A/7$) [14] and by using the alternate parameterization of Gilbert and Cameron [15]. A maximum variation of about 10% was obtained in the multiplicities. This is consistent with the idea that, for very proton (neutron) rich systems, the compound nucleus will preferentially emit protons (neutrons) so the predicted multiplicity is more stable than in situations where the nucleus has more options for decay. In the present case, the ^{66}As compound system is near the proton drip line and the predicted proton, α-particle, and neutron multiplicities at E_{cm} = 22 MeV are 2.38, 0.50, and 0.13, respectively. The fusion cross sections determined from the α-particle yields were consistent with those from the proton data but had larger error bars. Considering these observations, it is possible that the fusion cross sections quoted here could be up to 10% larger or 5% smaller than the true values. The experimental fusion excitation

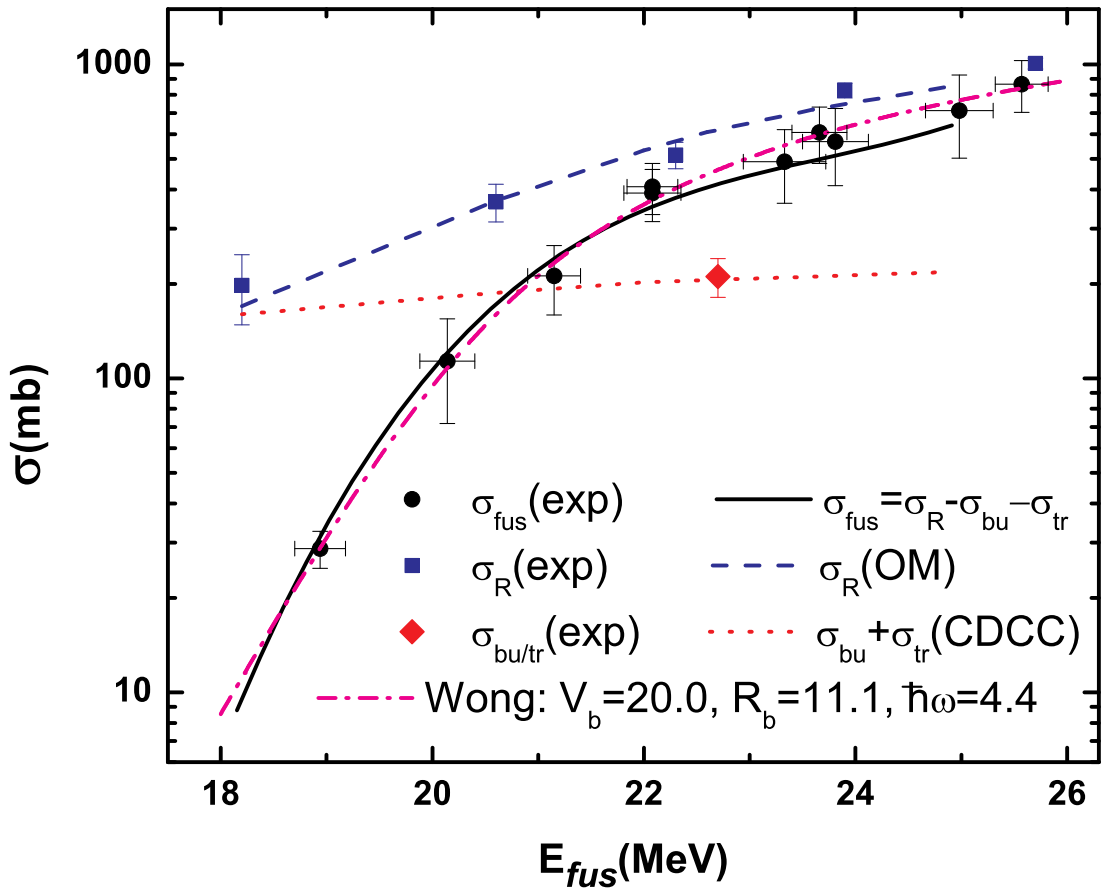

FIG. 2: Fusion excitation function σ_{fus} obtained in the present work. Data previously reported for the total reaction cross section σ_R [7] and the breakup cross section σ_{bu} [6, 7] are also shown. The horizontal error bars illustrate the energy averaging interval corresponding to the beam energy resolution (energy straggling effects are negligible). The dot-dashed curve is a Wong-model fit to the fusion data, yielding the indicated barrier parameters. The remaining curves were obtained from CDCC calculations performed with the code FRESCO.

function is represented by the filled circles in Fig. 2. The reported energies were determined iteratively and include a correction for mean energy loss in the target obtained by using successive Wong-model [16] fits to the data as weighting functions.

Strictly speaking, the fusion cross sections reported here are based on the assumption that complete fusion (CF) is the only mechanism responsible for the observed proton yields.

One concern is the possibility of having incomplete fusion (ICF), where the residual ^{7}Be after projectile breakup is absorbed by the target. For a given energy E, the effect of this process on the extracted cross sections depends on the factor f=CF/(CF+ICF) and on the ratio of the corresponding proton multiplicities $r(\mathrm{E}) = \mathrm{M}_p(^7\mathrm{Be})/\mathrm{M}_p(^8\mathrm{B})$. If r(E)=1 for all E, the reported values of σ_{fus} would correspond to total fusion (TF = CF+ICF). Estimations based on PACE calculations indicate that r(E) is actually an increasing function of E such that, for the experimental energy range, $0.72 \leq r(\mathrm{E}) \leq 0.85$. As a result, the effect of ICF is more important at lower energies. A value f=0.7 would have a negligible effect on σ_{fus} for all values of E as long as the fusion cross section is associated with TF. Even a factor as small as f=0.5 would leave the values of σ_{fus} within the reported error bars for all energies except the lowest one, where σ_{fus} would increase by 20% (the respective error bar is 14%). Similar results are obtained for ^{4}He or ^{3}He capture. The correction factors are somewhat larger in these cases, but it is worth noting that the already large cross sections will always be increased if there is substantial ICF since the proton multiplicities for ICF are always smaller than for CF. Note also that the measured total reaction cross section places an upper bound on σ_{fus}. Therefore, while we cannot rule out the ICF possibility, this will not substantially change the reported values of σ_{fus} as long as they are taken to refer to total fusion.

The final Wong-model fit to the data (dot-dashed curve in Fig. 2) yields 20.0 MeV and 11.1 fm for the barrier height and radius, respectively. From the systematics in the literature [17, 18], values of 20.8 MeV and 8.8 fm would be expected for these quantities in the case of normal systems. For the present halo system, the barrier height is shifted downward by 0.8 MeV and, most strikingly, the radius is 26% larger than normal. Such a big barrier radius could perhaps be attributed to a static effect due to the extended size of the proton halo, which enhances the total reaction probability throughout the entire energy range. The astonishing fact is that this larger total reaction cross section favors fusion in the proton-halo case.

The situation is quite different for the corresponding neutron-halo system ^{6}He+^{209}Bi. The systematics of Ref. [19] show that the reduced σ_R(E) for reactions involving a ^{6}He projectile is enhanced by nearly 70% with respect to the same quantity for reactions with ^{4}He, throughout the whole energy range. However, when the reduced fusion cross sections for the systems ^{4,6}He+^{209}Bi were compared with each other, they were relatively similar[20].

It seems, therefore, that the the extra total reaction cross section is depleted by transfer/breakup rather than fusion in the neutron halo case.

Figure 2 also shows the experimental data for the total reaction cross section σ_R [7] and transfer/breakup cross section $\sigma_{bu/tr}$ [6, 7], along with optical model and CDCC calculations[9] performed with the code FRESCO. The dotted curve includes full inelastic couplings in the continuum (bu), and also direct proton transfer (tr) calculated in the coupled-reaction-channel (CRC) approach. However, the calculated direct proton transfer cross section was only $\approx 5\%$ of the transfer/breakup yield. The solid curve is a calculation for total fusion assuming that $\sigma_{fus} = \sigma_R$ - σ_{bu}. The agreement with the present data is excellent, so for all practical purposes one can safely say that the sum of the total fusion and breakup yields exhausts the total reaction cross section. It is worth mentioning that the static effects on fusion discussed above do not exclude the possibility of dynamic effects induced by the breakup couplings. There could be, e.g., additional enhancement in the sub-barrier region due to these couplings. Within the simple framework of Wong's model, such an effect would be consistent with the relatively large value obtained for $\hbar\omega$ (4.4 MeV) in the present work. As discussed in Ref.[19], a large value of $\hbar\omega$ is likely a signature of dynamic sub-barrier enhancement.

In summary, fusion cross sections for the ^{8}B + ^{58}Ni system were extracted from evaporation proton measurements at nine near-barrier energies. The barrier radius inferred from the fusion data (11.1 fm) is 26% larger than that expected for normal systems, indicating a strong static effect of the ^{8}B proton halo. This is in contrast with previous observations for the neutron halo projectile ^{6}He, where a strong size effect of the halo is evident in the total reaction cross section data but not in the fusion yield. In both cases, however, the sum of the fusion and transfer/breakup channels exhausts the total reaction yield. It therefore appears that the halo wavefunction enhances the transfer/breakup process for neutron-halo systems and the fusion yield for proton-halo systems. One might speculate that this difference results from the different role played by Coulomb polarization in the case of a charged rather than a neutral halo.

This work has been partially supported by CONACYT (México) and by the US NSF under Grant No. PHY09-69456.

[1] L.F. Canto, P.R.S. Gomes, R. Donangelo, and M.S. Hussein, *Phys. Rep.* **424**, 1 (2006).

[2] N. Keeley, R. Raabe, N. Alamanos, and J. L. Sida, *Prog. Part. Nucl. Phys.* **59**, 579 (2007).

[3] N. Keeley, N. Alamanos, K. Kemper, and K. Rusek, *Prog. Part. Nucl. Phys.* **63**, 396 (2009).

[4] E. F. Aguilera, *et al.*, *Phys. Rev. Lett.* **84**, 5058 (2000).

[5] E. F. Aguilera, *et al.*, *Phys. Rev. C* **63**, 061603(R) (2001).

[6] V. Guimarães, *et al.*, *Phys. Rev. Lett.* **84**, 1862 (2000).

[7] E. F. Aguilera, *et al.*,*Phys. Rev. C* **79**, 021601(R) (2009).

[8] J. J. Kolata, *et al.*, *Phys. Rev. C* **75**, 031302(R) (2007).

[9] T. L. Belyaeva, E. F. Aguilera, E. Martinez-Quiroz, A. M. Moro, and J. J. Kolata, *Phys. Rev. C* **80**, 064617 (2009).

[10] E. F. Aguilera, *et al.*, Rev. Mex. Fís. **S52**, 41 (2006).

[11] M. Y. Lee, *et al.*, *Nucl. Instr. Meth.*, **A422**, 536 (1999).

[12] J.A. Tostevin, F.M. Nunes, and I.J. Thompson, *Phys. Rev. C* **63**, 024617 (2001).

[13] A. Gavron, *Phys. Rev. C* **21**, 230 (1980).

[14] R. G. Stokstad, Treatise on Heavy-Ion Science, vol. 3, Ed. D. A. Bromley (1985) p.83.

[15] A. Gilbert and A. G. W. Cameron, *Can. J. Phys.* **43**, 1446 (1965).

[16] C. Y. Wong, *Phys. Rev. Lett.* **31**, 766 (1973).

[17] L. C. Vaz, J. M. Alexander, and G. R. Satchler, *Phys. Rep.* **69**, 373 (1981).

[18] R. K. Puri and R. K. Gupta in *Heavy Ion Fusion: Exploring the Variety of Nuclear Properties; Proc. Int. Conf.: Padova, 1994,* edited by A. M. Stefanini, G. Nebbia, S. Lunardi, G. Montagnoli, and A. Vitturi (World Scientific, Singapore, 1994), p. 319.

[19] E. F. Aguilera, I. Martel, A. M. Sánchez-Benítez, and L. Acosta, *Phys. Rev. C* **83**, 021601(R) (2011).

[20] E. F. Aguilera, J. J. Kolata, and L. Acosta, *Phys. Rev. C* **81**, 011604(R) (2010).